POLARIZED RADIO EMISSION FROM FIVE SUPERNOVA REMNANTS

By D. K. Milne*

[Manuscript received 13 August 1971]

Abstract

Maps are presented of the polarization and total power emission at 2700 MHz from five southern supernova remnants: MSH 09−*32*, 10−*53*, 14−*63*, 15−*52*, and 15−*56*. Observations of 14−*63* and 15−*56* at 1410 MHz are also presented.

I. Introduction

Linear polarization has been detected in the radiofrequency emission from most supernova remnants. For 10 of the better resolved remnants, detailed maps of the polarization and magnetic field distributions over the radio sources have been published (Mayer and Hollinger 1968; Milne 1968, 1971*a*, 1971*b*; Kundu 1969, 1970, 1971; Kundu and Velusamy 1969, 1971; Baldwin *et al.* 1970; Milne and Wilson 1971; Weiler and Seielstad 1971).

This paper presents 2700 MHz polarization maps of five supernova remnants with supporting observations at 1410 MHz for two of them. The observations were all carried out with the Parkes 64 m radio telescope. Although previous polarization measurements have been made at the source peaks for three of the above remnants (Gardner, Morris, and Whiteoak 1969; Gardner, Whiteoak, and Morris 1969), detailed polarization maps have not been published for any of them. The present observations are a continuation of earlier 2700 MHz observations on IC 443 and Puppis A (Milne 1971*a*), MSH 14−4*15* (SN 1006 AD) (Milne 1971*b*), and Milne 56 (Milne and Dickel 1971).

II. Observations

(*a*) *2700 MHz Observations*

The 2700 MHz parametric correlation receiver (Batchelor, Brooks, and Cooper 1968) was used in the polarization mode, correlating the signals from two orthogonal probes in a circular waveguide antenna feed. The sum of the signals from the two orthogonal probes gives the total power output, while the crosscorrelation of the signals gives one of the linear Stokes parameters. By taking two declination scans with the feed rotated to position angles separated by 45° two independent linear Stokes parameters are obtained. To increase the accuracy of the observations a second pair of scans was made with the feed set at the orthogonal pair of position angles. A typical set of scans is shown in Figure 1. Such scans were made at right ascensions separated by approximately half beamwidths. These were then combined to produce the distributions of polarization ***E*** vectors shown in Figures 2 and 3. The polarization detection limit due to noise fluctuation for an observation using the set of four scans was about 0·01 KT_b, while for polarization temperatures greater

* Division of Radiophysics, CSIRO, P.O. Box 76, Epping, N.S.W. 2121.

than $0 \cdot 03$ K the probable error in position angle was less than $\pm 10°$. The isotherms shown in Figure 3 were constructed from the average of the four total power records. The background has been removed from each total power map by subtracting a sloping linear baselevel from each declination scan. The value of the baselevel at the centre of the source is given in the figure captions.

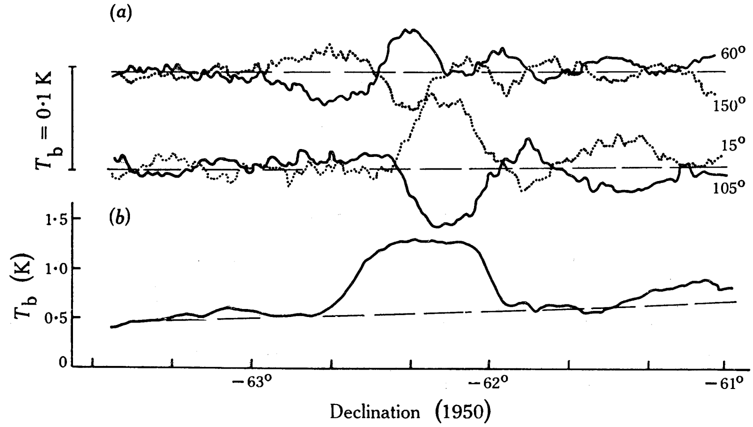

Fig. 1.—Declination scans through MSH 14−6*3* at R.A. $14^{h}40^{m}52^{s}$ (1950), comprising (*a*) four scans of polarization brightness temperature at the indicated position angles, together with (*b*) one of the four total power records. The adopted baselevels are shown by dashed lines. The difficulties experienced in cancelling the background polarization can be appreciated from this figure.

Calibration scans were made on the unpolarized radio source Hydra A, for which a flux density of 23 f.u.* was assumed. The brightness temperature scale and the telescope beamwidth ($8' \cdot 4$ arc) were determined from these scans. A polarization map of this source is given in Figure 2(*a*). The polarization shown is spurious and is due in part to two instrumental effects:

(1) A variation in antenna gain with rotation of the feed. This effect was found to introduce a spurious polarization of $0 \cdot 5\%$ fixed in direction relative to the altazimuth coordinate system of the telescope.

(2) An effect related to the gradient of the measured brightness distribution. This is caused by the polarization dependence of the beam ellipticity and squint, and is apparent when the feed is rotated on the steep sides of a source. For the present observations the spurious polarization intensity (in kelvin) due to this effect is approximately $0 \cdot 03$ multiplied by the brightness temperature gradient (in kelvin per minute of arc) and is directed along the maximum gradient.

The spurious polarization over Hydra A is shown uncorrected in Figure 2(*a*), corrected for the first effect in Figure 2(*b*), and approximately corrected for both effects in Figure 2(*c*). The corrections are not ideal and there still remains some spurious polarization on the source, particularly on the western side. In addition, between one and two beamwidths from the centre of the source there is weak polarization

* 1 flux unit (f.u.) = $10^{-26}\,W\,m^{-2}\,Hz^{-1}$.

(less than 0·5% of the peak temperature) directed mainly transverse to the radius vector to the source. The magnitude of the corrections and the residual spurious polarization can be gauged from a comparison of these figures. The 2700 MHz maps in Figure 3 have been approximately corrected for both effects (1) and (2) above.

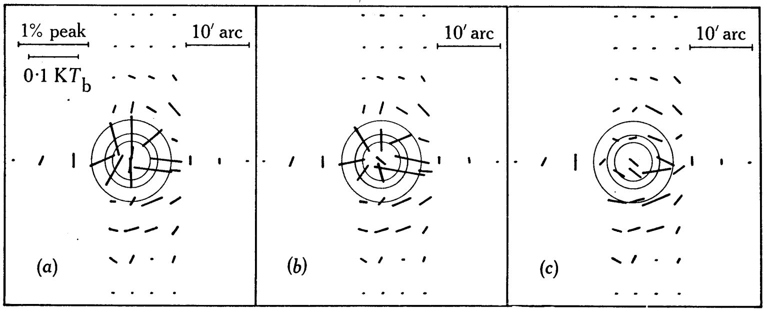

Fig. 2.—Distribution of spurious polarization $\boldsymbol{E}$ vectors over the unpolarized point source Hydra A for the polarization data (*a*) unprocessed, (*b*) processed to remove the gain effect (1) (see text), and (*c*) processed to remove the gradient effect (2) also. The peak total power temperature is 16 K and one-quarter, one-half, and three-quarter power isotherms are shown.

In addition to these instrumental effects there is generally a polarized component in the background emission. This adds considerable uncertainty to the source polarization of objects as large in angular size as these five remnants. Although not

Table 1

FLUX DENSITIES AND SPECTRAL INDICES FOR FIVE SUPERNOVA REMNANTS

MSH source number	Galactic source number	Flux density (f.u.)* 86	408	1410	1660	2650	2700	5000 MHz	Spectral index
09−32	G260·4−3·4	25[1]	12·8[2]	8[3] 10[2]		7[3]	7·4[4]		−0·37
10−53	G284·2−1·8	71[1]		21[5]			16[4]		−0·46
14−63	G315·4−2·3	110[1]		30[3] 25[4]		20[3]	22[4]		−0·49
15−52 A	G320·3−1·0		50[6] 30[7]	28[5]	29·5[8]		23[4] 23[9]		−0·6
B	G320·3−1·4		46[6]	18[5]	19[8]		18[4] 12[9]		−0·6
A+B	G320·3−1·2	252(190)[1]	94[6]	46[5]	48·5[8]		41[4] 35[9]		−0·6
15−56	G326·2−1·7	323(270)[1]	170[7]	129[3] 135[4]		115[3]		98[10]	−0·26

* References: (1) Mills, Slee, and Hill (1960, 1961); (2) Bolton, Gardner, and Mackey (1964); (3) Hill (1967); (4) present work; (5) isotherms from Hill (1968) integrated by present author; (6) Shaver and Goss (1970); (7) Kesteven (1968); (8) Milne *et al.* (1969); (9) Day, Thomas, and Goss (1969); (10) Milne (1969).

shown in Figure 3, the scans were continued well to the north and south of each source, and the baselevels of the polarization scans were adjusted to cancel, as near as possible, any background polarization in these portions of the scans. The

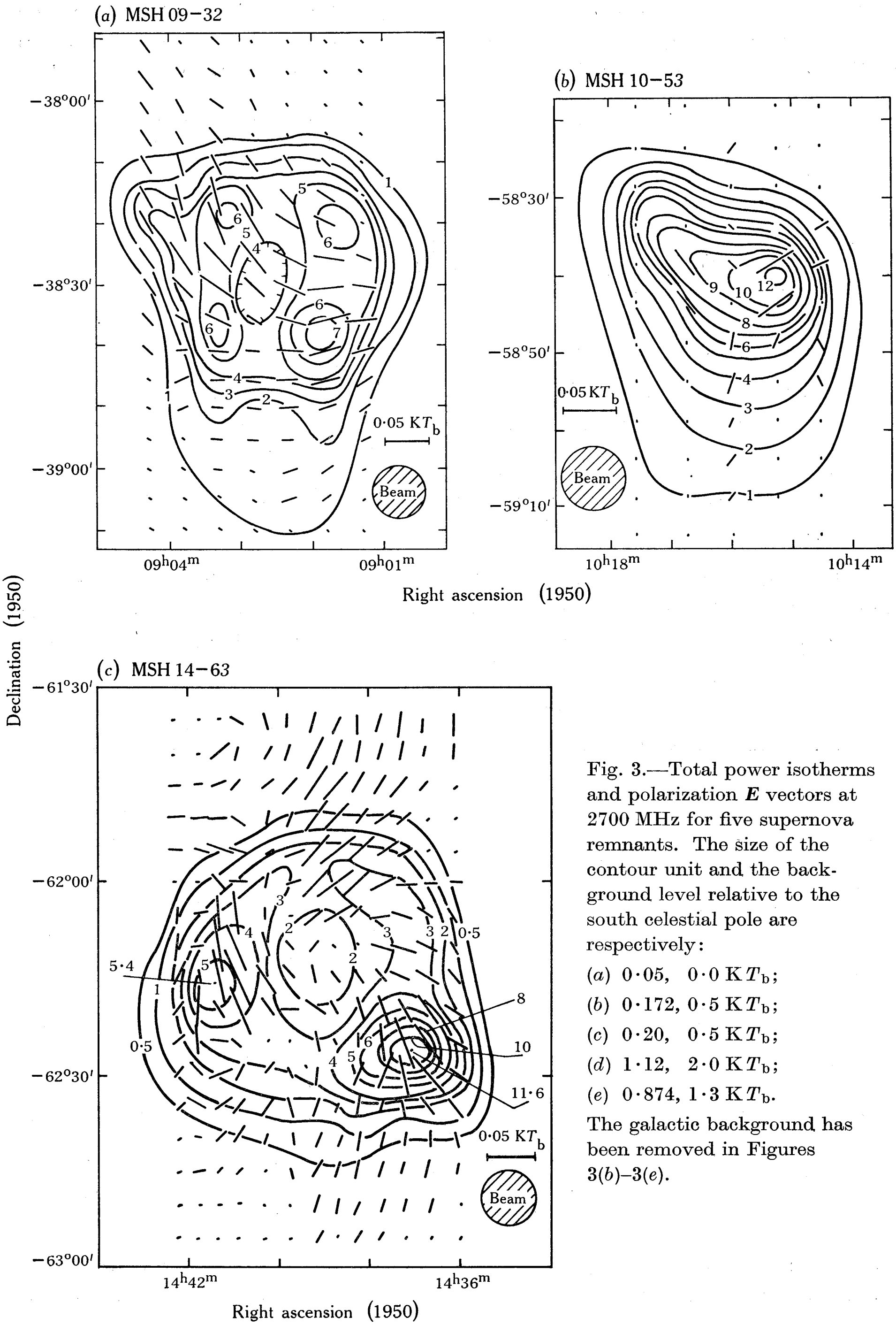

Fig. 3.—Total power isotherms and polarization $\boldsymbol{E}$ vectors at 2700 MHz for five supernova remnants. The size of the contour unit and the background level relative to the south celestial pole are respectively:

(*a*) 0·05, 0·0 KT_b;

(*b*) 0·172, 0·5 KT_b;

(*c*) 0·20, 0·5 KT_b;

(*d*) 1·12, 2·0 KT_b;

(*e*) 0·874, 1·3 KT_b.

The galactic background has been removed in Figures 3(*b*)–3(*e*).

polarization was usually found to be constant in the regions scanned beyond the boundaries of the maps shown in Figure 3, so that adoption of zero polarization in these regions seemed to be the best method of fixing the polarization baseline. The difficulties in the choice of baselevels for the polarization scans can be appreciated from an examination of the scans shown in Figure 1. These clearly indicate that there is not only a polarized component in the emission from the supernova remnant

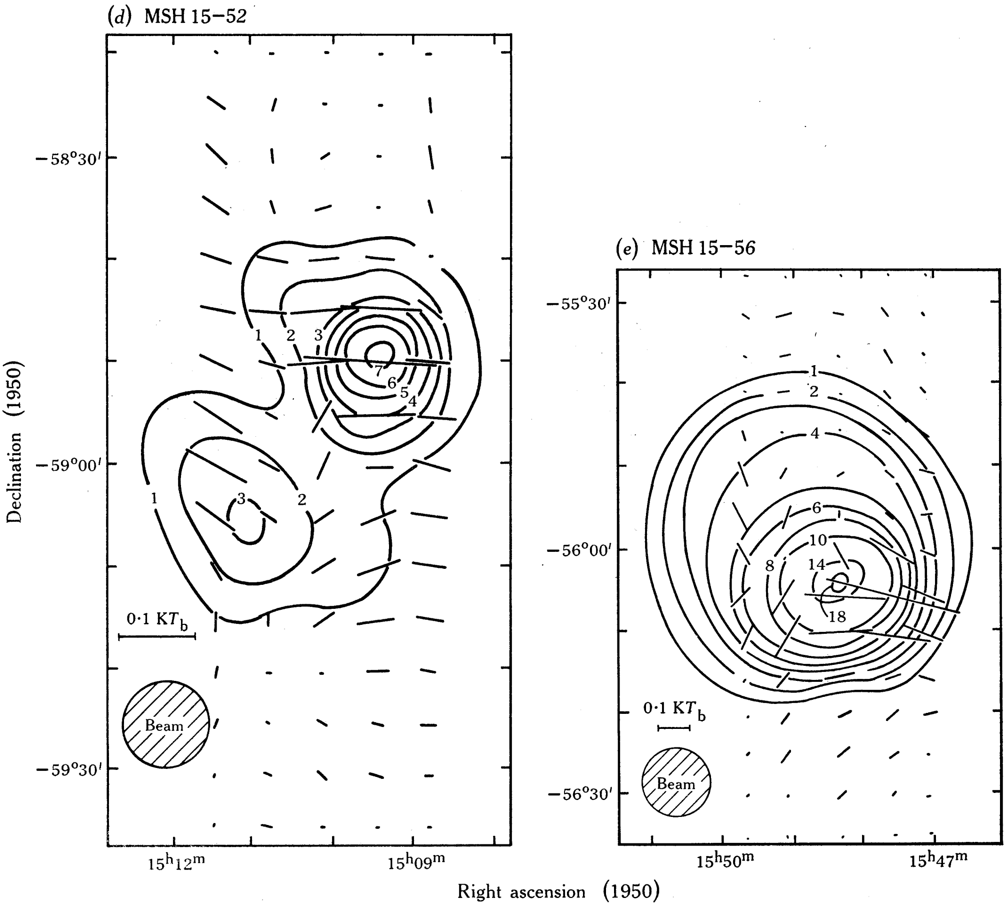

Figs. 3(*d*) and 3(*e*).

MSH 14−63, but also considerable polarization beyond the source, particularly to the north, which is in the direction of the galactic plane.

The total power contours were integrated to obtain flux densities for each remnant and the results are given in Table 1, together with the 1410 MHz values obtained from the observations described in Section II(*b*). The table also lists values obtained by other observers at frequencies between 86 and 5000 MHz. The power law spectral indices that best fit all these values are given in the final column of the table.

(*b*) *1410 MHz Observations*

The 1410 MHz isotherms and polarization $\boldsymbol{E}$ vectors for MSH 14−*63* and 15−*56* are displayed in Figures 4(*a*) and 4(*b*). These were obtained using observational techniques similar to those employed at 2700 MHz. Further details of the receiving system are given by Milne (1971*b*). At 1410 MHz the half-power beamwidth is 15′·3 and the former instrumental effects are negligible. Consequently no corrections for spurious polarization were made to the data in Figure 4. The present 1410 MHz integrated flux densities for MSH 14–*63* and 15−*56* as given in Table 1 are based on a flux density of 42 f.u. for the calibration source Hydra A.

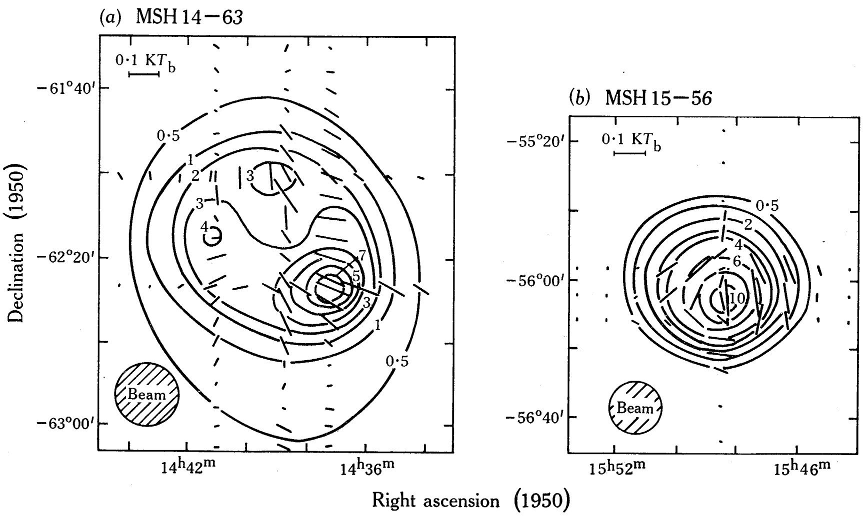

Fig. 4.—Total power isotherms and polarization $\boldsymbol{E}$ vectors at 1410 MHz for two supernova remnants. The size of the contour unit and the approximate background level relative to the south celestial pole are respectively: (*a*) 0·6, 1·6 KT_b; (*b*) 3·12, 1·9 KT_b. The galactic background has been removed from both maps.

III. Discussion

With the exception of MSH 15−*56*, each of the present objects is of low radio surface brightness, with much of the source intensity commensurate with that of the background. Also the observations are complicated by the presence of a polarized component in the background emission. Nevertheless there is clearly polarization associated with each of the sources, but it is superimposed on the background polarization.

A different choice of baselevels for the polarization scans would remove the off-source polarization shown in Figures 3 and 4, although this would increase the polarization in the region scanned beyond the boundaries of the figures. It is also possible that the off-source polarization shown near the source is in fact associated with the supernova remnant. This is seen in IC 443 and Puppis A (Milne 1971*a*) and in Milne 56 at 5000 MHz (Milne and Dickel 1971), where the adoption of the best baselevels over long off-source portions of the scans results in residual polarization close to, but outside, the remnants. Certainly the polarization distributions shown in Figures 3(*a*), 3(*c*), and 3(*d*) suggest that polarized "spurs" extend beyond these sources. These might be caused by a leakage of cosmic ray electrons from the remnant, as Baldwin (1967) has suggested for the flares outside the shell of Cassiopea A.

From the observations presented here it is not possible to suggest directions for the magnetic field in the sources. The 5000 MHz polarization maps of these five supernova remnants, together with maps of several others, will be presented in a later paper (Milne and Dickel, in preparation), in which a discussion of the polarization and magnetic field distributions will be given.

IV. Acknowledgments

The author is grateful to Dr. J. A. Roberts and Dr. J. L. Caswell for discussion of the manuscript.

V. References

Baldwin, J. E. (1967).—*In* "Radio Astronomy and the Galactic System". (Ed. H. Van Woerden.) p. 337. (Academic Press: London.)

Baldwin, J. E., Jennings, J. E., Shakeshaft, J. R., Warner, P. O., Wilson, D. M. A., and Wright, M. C. H. (1970).—*Mon. Not. R. astr. Soc.* **150**, 253.

Batchelor, R. A., Brooks, J. W., and Cooper, B. F. C. (1968).—*IEEE Trans. Antennas Propag.* AP **16**, 228.

Bolton, J. G., Gardner, F. F., and Mackey, M. B. (1964).—*Aust. J. Phys.* **17**, 340.

Day, G. A., Thomas, B. MacA., and Goss, W. M. (1969).—*Aust. J. Phys. astrophys. Suppl.* No. 11, 11.

Gardner, F. F., Morris, D., and Whiteoak, J. B. (1969).—*Aust. J. Phys.* **22**, 79.

Gardner, F. F., Whiteoak, J. B., and Morris, D. (1969).—*Aust. J. Phys.* **22**, 821.

Hill, E. R. (1967).—*Aust. J. Phys.* **20**, 297.

Hill, E. R. (1968).—*Aust. J. Phys.* **21**, 735.

Kesteven, M. J. L. (1968).—*Aust. J. Phys.* **21**, 369.

Kundu, M. R. (1969).—*Astrophys. J. Lett.* **158**, L103.

Kundu, M. R. (1970).—*Astrophys. J.* **162**, 17.

Kundu, M. R. (1971).—*Astrophys. J. Lett.* **165**, L55.

Kundu, M. R., and Velusamy, T. (1969).—*Astrophys. J.* **155**, 807.

Kundu, M. R., and Velusamy, T. (1971).—*Astrophys J* **163**, 231.

Mayer, C. H., and Hollinger, J. P. (1968).—*Astrophys. J.* **151**, 53.

Mills, B. Y., Slee, O. B., and Hill, E. R. (1960).—*Aust. J. Phys.* **13**, 676.

Mills, B. Y., Slee, O. B., and Hill, E. R. (1961).—*Aust. J. Phys.* **14**, 497.

Milne, D. K. (1968).—*Aust. J. Phys.* **21**, 201.

Milne, D. K. (1969).—*Aust. J. Phys.* **22**, 613.

Milne, D. K. (1971*a*).—*Aust. J. Phys.* **24**, 429.

Milne, D. K. (1971*b*).—*Aust. J. Phys.* **24**, 757.

Milne, D. K., and Dickel, J. R. (1971).—*Nature, Lond.* **231**, 33.

Milne, D. K., and Wilson, T. L. (1971).—*Astr. Astrophys.* **10**, 220.

Milne, D. K., Wilson, T. L., Gardner, F. F., and Mezger, P. G. (1969).—*Astrophys. Lett.* **4**, 96.

Shaver, P. A., and Goss, W. M. (1970).—*Aust. J. Phys. astrophys. Suppl.* No. 14, 76.

Weiler, K. W., and Seielstad, G. A. (1971).—*Astrophys. J.* **163**, 455.